EPJ Web of Conferences **353**, 01003 (2026) https://doi.org/10.1051/epjconf/202635301003
mm Universe 2025

Blind detection of galaxy clusters in the COSMOS field via the SZ effect

D. Chérouvrier[1], R. Adam[2], P. Ade[3], H. Ajeddig[4], S. Amarantidis[5], P. André[4], H. Aussel[4], R. Barrena[6,7], A. Beelen[8], A. Benoît[9], S. Berta[10], M. Béthermin[11,8], A. Bongiovanni[5], J. Bounmy[1], O. Bourrion[1], L. -J. Bing[12], M. Calvo[9], A. Catalano[1], M. De Petris[13], F. X. Désert[14], S. Doyle[3], E. F. C. Driessen[10], G. Ejlali[15], A. Ferragamo[13], M. Fernández-Torreiro[1], A. Gomez[16], J. Goupy[9], C. Hanser[1], S. Katsioli[17,18], F. Kéruzoré[19], C. Kramer[10], B. Ladjelate[5], G. Lagache[8], S. Leclercq[10], J.-F. Lestrade[20], J. F. Macías-Pérez[1], S. C. Madden[4], A. Maury[21,22,4], F. Mayet[1], J. -B. Melin[23], A. Monfardini[9], A. Moyer-Anin[1], M. Muñoz-Echeverría[24], I. Myserlis[5], R. Neri[10], A. Paliwal[25], L. Perotto[1], G. Pisano[13], E. Pointecouteau[24], N. Ponthieu[14,8], G. W. Pratt[4], V. Revéret[4], A. J. Rigby[26], A. Ritacco[1], H. Roussel[27], F. Ruppin[28], M. Sánchez-Portal[5], S. Savorgnano[1], K. Schuster[10], A. Sievers[5], C. Tucker[3], and R. Zylka[10]

[1]Univ. Grenoble Alpes, CNRS, Grenoble INP, LPSC-IN2P3, 53, avenue des Martyrs, 38000 Grenoble, France
[2]Université Côte d'Azur, Observatoire de la Côte d'Azur, CNRS, Laboratoire Lagrange, France
[3]School of Physics and Astronomy, Cardiff University, Queen's Buildings, The Parade, Cardiff, CF24 3AA, UK
[4]Université Paris-Saclay, Université Paris Cité, CEA, CNRS, AIM, F-91191, Gif-sur-Yvette, France
[5]Institut de Radioastronomie Millimétrique (IRAM), Avenida Divina Pastora 7, Local 20, E-18012, Granada, Spain
[6]Instituto de Astrofísica de Canarias, C/ Vía Láctea s/n, E-38205 La Laguna, Tenerife, Spain
[7]Universidad de La Laguna, Departamento de Astrofísica, E-38206 La Laguna, Tenerife, Spain
[8]Aix Marseille Univ, CNRS, CNES, LAM (Laboratoire d'Astrophysique de Marseille), Marseille, France
[9]Institut Néel, CNRS, Université Grenoble Alpes, France
[10]Institut de Radioastronomie Millimétrique (IRAM), 300 rue de la Piscine, 38400 Saint-Martin-d'Hères, France
[11]Université de Strasbourg, CNRS, Observatoire astronomique de Strasbourg, UMR 7550, 67000 Strasbourg, France
[12]Astronomy Centre, Department of Physics and Astronomy, University of Sussex, Brighton BN1 9QH
[13]Dipartimento di Fisica, Sapienza Università di Roma, Piazzale Aldo Moro 5, I-00185 Roma, Italy
[14]Univ. Grenoble Alpes, CNRS, IPAG, 38000 Grenoble, France
[15]Institute for Research in Fundamental Sciences (IPM), School of Astronomy, Tehran, Iran
[16]Centro de Astrobiología (CSIC-INTA), Torrejón de Ardoz, 28850 Madrid, Spain
[17]National Observatory of Athens, Institute for Astronomy, Astrophysics, Space Applications and Remote Sensing, Ioannou Metaxa and Vasileos Pavlou GR-15236, Athens, Greece
[18]Department of Astrophysics, Astronomy & Mechanics, Faculty of Physics, University of Athens, Panepistimiopolis, GR-15784 Zografos, Athens, Greece
[19]High Energy Physics Division, Argonne National Laboratory, 9700 South Cass Avenue, Lemont, IL 60439, USA
[20]LERMA, Observatoire de Paris, PSL Research University, CNRS, Sorbonne Université, UPMC, 75014 Paris, France

[21]Institute of Space Sciences (ICE), CSIC, Campus UAB, Carrer de Can Magrans s/n, E-08193, Barcelona, Spain
[22]ICREA, Pg. Lluís Companys 23, Barcelona, Spain
[23]Université Paris-Saclay, CEA, Département de Physique des Particules, 91191, Gif-sur-Yvette, France
[24]IRAP, CNRS, Université de Toulouse, CNES, UT3-UPS, (Toulouse), France
[25]Dipartimento di Fisica, Università di Roma 'Tor Vergata', Via della Ricerca Scientifica 1, I-00133 Roma, Italy
[26]School of Physics and Astronomy, University of Leeds, Leeds LS2 9JT, UK
[27]Institut d'Astrophysique de Paris, CNRS (UMR7095), 98 bis boulevard Arago, 75014 Paris, France
[28]University of Lyon, UCB Lyon 1, CNRS/IN2P3, IP2I, 69622 Villeurbanne, France

Abstract. Clusters of galaxies are powerful cosmological probes, and the thermal Sunyaev Zel'dovich (tSZ) effect provides an efficient method for their detection. High-angular-resolution observations, such as those provided by the NIKA2 camera on the IRAM 30-m telescope, are essential to target low mass and high-redshift clusters. We performed a blind search for galaxy clusters in the COSMOS field using 150 GHz data from the NIKA2 Cosmological Legacy Survey. We applied a matched-filter technique based on a universal pressure profile to extract cluster candidates. The purity and completeness of the sample were assessed using realistic simulations. We detected 16 cluster candidates above an S/N of 4, eight of which have confirmed counterparts.

1 Introduction

Galaxy clusters, formed in the latest stages of structure formation, are unique cosmological probes to study structure formation and its evolution [1, 2]. Their detection is a major field of research in modern cosmology, with a need to observe large samples of clusters to further reduce uncertainties on cosmological parameters. Large cluster catalogs have been built over the last decades at different wavelengths, from optical surveys to X-ray observations. The thermal Sunyaev-Zel'dovich effect (tSZ) [3] was first detected in the 1970s [4]. Since then, observations at millimeter wavelengths have emerged as a great tool for the detection and study of galaxy clusters. The *Planck* satellite [5], the South Pole Telescope (SPT) [6] and the Atacama Cosmology Telescope (ACT) [7] have detected hundreds to thousands of clusters over large fractions of the sky. However, these surveys are limited by their angular resolution, which makes the detection of high-redshift low-mass clusters challenging. As a consequence, there is a need for high angular resolution instruments (tens of arcseconds) in order to map the SZ signal for high redshift and/or low-mass clusters of galaxies. Clusters in this mass-redshift regime are expected to be of great cosmological interest [8], especially to verify our current understanding of structure formation.

In this context, the NIKA2 camera [9–11] installed at the IRAM 30-m telescope is well-suited for tSZ studies. As part of the NIKA2 Cosmological Legacy Survey (N2CLS), 195 hours of deep observations of the COSMOS field have been obtained, providing an opportunity to search for galaxy clusters in a region with extensive multi-wavelength coverage. We review the results presented in more detail in [12]. In this paper, all masses are expressed using the quantity M_{500}, which represents the mass contained within a radius R_{500}, where the average density equals 500 times the critical density at the cluster redshift.

2 Cluster detection

We searched for galaxy clusters in the NIKA2 COSMOS 150 GHz map using a matched-filter technique optimized for the tSZ signal. The filter is constructed from a model of the expected tSZ surface brightness profile, convolved with the instrument beam and corrected for the pipeline transfer function, to maximize sensitivity to cluster-like features. Cluster candidates were identified as peaks above a signal-to-noise ratio (S/N) threshold of 4 in the filtered maps, after masking bright point sources to avoid contamination. This approach yielded 16 cluster candidates in the central low-noise region of the map. The mean S/N of our candidate sample is S/N $\sim$ 4.51, with candidates appearing as compact negative features in the signal map, consistent with the expected tSZ signature. We show in Figure 1 one of the S/N maps, filtered to optimally extract objects with angular size $\theta_{500} = 30.4''$. Positive peaks in this map, highlighted in black, can be identified as cluster candidates. The 16 cluster candidates and their main properties are given in Table 1.

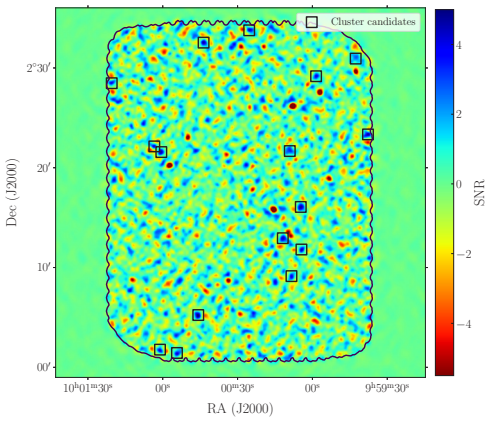

Figure 1. S/N map of the matched-filtered 2 mm COSMOS map. Positive S/N values corresponding to cluster candidates are shown in blue and circled by black squares. The angular size of the applied matched filter is equal to 30.4″. The black contour shows the high quality region. 16 candidates have been detected above a S/N threshold of 4.

Candidate Name	RA	DEC	S/N	z	θ_{500}	Y_{500}	M_{500}	Matching cluster name	Reference(s)
	°	°			arcmin	10^{-5} arcmin^2	10^{14} $M_\odot$	(distance [″])	
NK2-CL J100045.8+020514.3	150.1907	2.0873	5.31	–	$0.74^{+0.40}_{-0.20}$	$1.60^{+1.45}_{-0.56}$	–	–	–
NK2-CL J095937.7+022320.4	149.9071	2.3890	5.00	0.74±0.03 (p)	$1.38^{+0.12}_{-0.13}$	$3.35^{+1.77}_{-1.34}$	$1.51^{+0.40}_{-0.38}$	ALH J0959.38+0223.03 (17.8″)	(1)
NK2-CL J100004.7+021604.4	150.0194	2.2679	4.97	–	$0.92^{+0.62}_{-0.29}$	$1.95^{+2.65}_{-0.88}$	–	–	–
NK2-CL J100043.6+023232.4	150.1818	2.5423	4.87	–	$0.65^{+0.31}_{-0.13}$	$1.11^{+0.75}_{-0.30}$	–	–	–
NK2-CL J100025.3+023346.4	150.1056	2.5629	4.67	0.72±0.02 (p)	$1.37^{+0.12}_{-0.14}$	$2.90^{+1.57}_{-1.24}$	$1.38^{+0.38}_{-0.37}$	[BMH2011] 124 (11.5″)	(2), (3), (4)
NK2-CL J100100.6+022134.4	150.2524	2.3596	4.67	0.77±0.01 (p)	$1.36^{+0.09}_{-0.11}$	$3.47^{+1.42}_{-1.25}$	$1.56^{+0.33}_{-0.34}$	[SCC2012] 0788 (9.1″)	(5)
NK2-CL J100004.4+021148.4	150.0183	2.1968	4.60	0.94±0.05 (s)	$1.10^{+0.09}_{-0.10}$	$2.10^{+0.91}_{-0.78}$	$1.21^{+0.27}_{-0.27}$	[KLI2009] 146 (8.7″)	(3)
NK2-CL J100103.4+022208.4	150.2641	2.3690	4.54	–	$0.59^{+0.23}_{-0.09}$	$0.85^{+0.35}_{-0.20}$	–	–	–
NK2-CL J100011.9+021256.5	150.0494	2.2157	4.48	0.24±0.08 (p)	$3.79^{+2.11}_{-1.01}$	$28.20^{+69.45}_{-16.79}$	$2.83^{+1.55}_{-0.88}$	XMMXCS J100012.3+021246.7 (11.7″)	(6)
NK2-CL J100101.1+020146.6	150.2546	2.0296	4.30	–	$0.71^{+0.44}_{-0.16}$	$0.96^{+0.83}_{-0.29}$	–	–	–
NK2-CL J100054.3+020126.4	150.2262	2.0240	4.28	1.42±0.01 (p)	$0.81^{+0.05}_{-0.06}$	$1.56^{+0.62}_{-0.53}$	$1.00^{+0.21}_{-0.21}$	[SCC2012] 1517 (16.0″)	(5)
NK2-CL J100009.1+022140.3	150.0378	2.3612	4.27	–	$2.56^{+2.96}_{-1.16}$	$14.30^{+81.99}_{-10.55}$	–	–	–
NK2-CL J095942.6+023056.5	149.9277	2.5157	4.08	0.73±0.02 (s)	$1.45^{+0.11}_{-0.13}$	$4.10^{+1.83}_{-1.55}$	$1.69^{+0.39}_{-0.39}$	DESI 2353000051 (12.0″)	(7)
NK2-CL J100120.5+022828.2	150.3353	2.4745	4.07	–	$0.71^{+0.44}_{-0.15}$	$0.93^{+0.75}_{-0.28}$	–	–	–
NK2-CL J100008.4+020908.3	150.0350	2.1523	4.04	–	$0.77^{+0.65}_{-0.21}$	$1.20^{+1.72}_{-0.44}$	–	–	–
NK2-CL J095958.5+022910.4	149.9938	2.4862	4.01	0.40±0.01 (p)	$2.52^{+0.22}_{-0.23}$	$12.24^{+6.22}_{-4.77}$	$2.38^{+0.61}_{-0.57}$	[SCC2012] 0270 (14,8″)	(5)

Table 1. Galaxy cluster candidates, sorted by decreasing S/N, with S/N > 4. The catalog gives the candidate's name, position, S/N, estimated redshift if matched, angular size θ_{500}, tSZ flux Y_{500}, and the name of the matched counterpart with its angular distance to the candidate.

3 Cluster detection characterization via simulations

To characterize our sample of cluster candidates, we produce realistic simulations containing the tSZ signal of galaxy clusters, noise from the null maps, and the Simulated Infrared Dusty Extragalactic Sky model (SIDES) [13, 14] to account for the signal expected from other sky components. We applied the detection algorithm to these simulated maps and identified all S/N peaks above a threshold of 4. On average, simulations yielded 26 ± 5 detections per map. In the COSMOS data, we found 16 detections with S/N > 4, which is lower but still compatible within 2σ with the simulations.

We then estimated the completeness and purity of our sample from these simulations, as shown in Figure 2. Completeness, defined as the fraction of true clusters detected, exceeds 80% for $M_{500} > 1.7 \times 10^{14} M_{\odot}$ across all redshifts. The detection algorithm is less efficient for low-mass, low-redshift clusters due to filtering during the data reduction process. Purity, which is the fraction of detections that are true clusters, rises quickly with S/N, reaching 80% at S/N ~ 5 and is higher for high-redshift clusters.

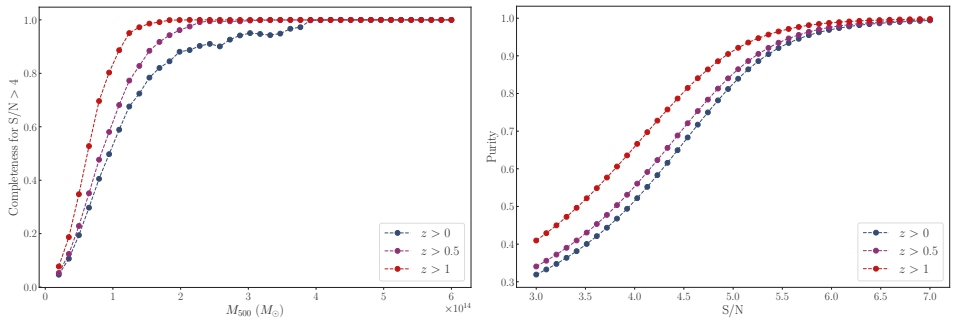

Figure 2. (Left): Completeness as a function of the mass, M_{500}, for different redshift ranges. (Right): Purity as a function of S/N for different redshift ranges.

4 Cluster candidates validation

We validated our cluster candidate sample by cross-matching with NED, SIMBAD, and VizieR, using a 20 $''$ search radius. This radius was validated with random association tests, showing that it yielded the best ratio between true and chance associations. Out of 16 candidates, 8 have counterparts in existing catalogs, mostly in optical/NIR surveys. The median redshift of matched clusters is $z \sim 0.74$, with two at $z > 0.9$.

To complement the validation process, we also examined spectroscopic [15] and photometric [16] redshift catalogs. We found that in most cases, the expected redshift for the identified NIKA2 candidates lies in the peak of the redshift distribution of galaxies. Some unmatched candidates also show well-defined redshift peaks at their position.

Finally, we checked that all known massive and bright clusters in the NIKA2 COSMOS footprint were detected in the NIKA2 COSMOS map. To confirm our survey's completeness as described in Section 3, we confirmed that all bright clusters are detected. Undetected clusters are low mass and/or low-redshift ones, where our completeness is very limited.

5 Properties of cluster candidates

To characterize the properties of each cluster candidate, we fitted their millimeter emission with a spherical tSZ model using MCMC analysis, allowing both mass and redshift to vary.

For candidates with known counterparts, literature redshifts were used as priors to improve constraints. As expected, a tighter redshift prior greatly improves the constraints. Mass estimates for matched clusters were derived from the MCMC fits and are shown in the left panel of Figure 3, which compares the mass-redshift distribution of our sample to other large SZ surveys. We see that our completeness contours are steeper at high redshifts compared to other surveys, as expected from NIKA2's compact beam. This is because the tSZ flux of distant (and compact) clusters is less affected by beam dilution, making it more sensitive to fainter, lower-mass clusters. The median mass of our sample is $M_{500} = 1.54^{+0.76}_{-0.30} \times 10^{14} M_{\odot}$. Overall, confirmed NIKA2 detections correspond to intermediate and high redshift, low-mass clusters, probing a similar region in the mass-redshift plane as the newest SPT-Deep catalog [17], which is currently the deepest tSZ cluster survey.

The right panel of Figure 3 presents the cluster surface density as a function of mass for the same surveys. These results highlight NIKA2's capabilities to complement existing surveys, especially at lower masses.

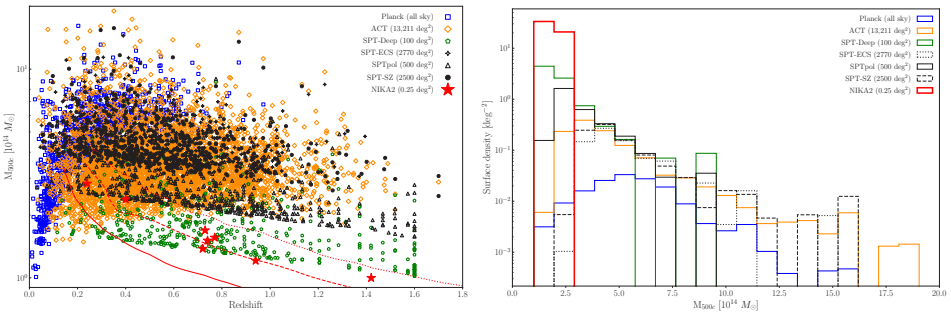

Figure 3. (Left): NIKA2 matched cluster sample in the mass-redshift plane. Cluster samples from other blind tSZ surveys such as PSZ2 [5], ACT DR5 [18], SPT-ECS [19], SPTpol [6], SPT-SZ [20], and SPT-Deep [17] are shown for comparison. The 20%, 50% and 80% completeness contours are shown as solid, dashed and dotted red lines, respectively. (Right): Cluster surface density as a function of cluster mass for the same surveys.

6 Conclusions

We have presented the first blind detection of galaxy clusters at mm wavelength via the tSZ effect at high angular resolution (18.5″) using the NIKA2 camera. 16 cluster candidates were identified above S/N > 4, and the detection threshold was validated with realistic simulations. The sample shows a completeness above 80% for $M_{500} > 1.7 \times 10^{14} M_{\odot}$ and a purity of about 50% at the chosen S/N threshold of 4. Eight candidates have counterparts in external catalogs, with a median redshift of $z \sim 0.74$. Reliable mass estimates were obtained for candidates with redshift information, with a median mass of $M_{500} = 1.54 \times 10^{14} M_{\odot}$. We showed that the NIKA2 camera is a very powerful instrument to blindly detect low-mass high-redshift galaxy clusters via the SZ effect. As the N2CLS survey was not optimized for this prospect, we expect that a dedicated NIKA2 cluster survey would greatly improve the number of detections.

Looking ahead, future upgrades of the NIKA2 camera are being planned to enhance its sensitivity and mapping speed by scaling up the number of detectors, as well as adding two new frequency bands at 90 and 230 GHz [21]. With these upgrades, a dedicated NIKA3 cluster survey could cover a much larger area and match the depth achieved by NIKA2, allowing for the detection of a significantly larger sample of clusters.

In addition, a new instrument that would be placed on a 13-m telescope is currently being

studied. The main goal of this new camera would be to cover a large fraction of the northern sky with a FoV of 1 deg and an angular resolution of about 1 arcmin at 90 GHz. The current survey strategy involves a wide survey covering 6000 deg^2 and a deep survey covering 300 deg^2.

Finally, follow-up observations of the most distant cluster candidate in the NIKA2 sample, NK2-CL J100054.3+020126.4 at $z = 1.42$, are being carried out with the NOEMA interferometer. With an angular resolution of about 5″ at 82 GHz, NOEMA is well suited to confirm the tSZ nature of this candidate and obtain a very high resolution tSZ map.

Acknowledgements

We would like to thank the IRAM staff for their support during the observation campaigns. The NIKA2 dilution cryostat has been designed and built at the Institut Néel. In particular, we acknowledge the crucial contribution of the Cryogenics Group, and in particular Gregory Garde, Henri Rodenas, Jean-Paul Leggeri, Philippe Camus. This work has been partially funded by the Foundation Nanoscience Grenoble and the LabEx FOCUS ANR-11-LABX-0013. This work is supported by the French National Research Agency under the contracts "MKIDS", "NIKA" and ANR-15-CE31-0017 and in the framework of the "Investissements d'avenir" program (ANR-15-IDEX-02). This work has been supported by the GIS KIDs. This work has benefited from the support of the European Research Council Advanced Grant ORISTARS under the European Union's Seventh Framework Programme (Grant agreement No. 291294). R. A. acknowledges support from the Programme National Cosmology et Galaxies (PNCG) of CNRS/INSU with INP and IN2P3, co-funded by CEA and CNES. R. A. was supported by the French government through the France 2030 investment plan managed by the National Research Agency (ANR), as part of the Initiative of Excellence of Université Côte d'Azur under reference number ANR-15-IDEX-01. A. Maury acknowledges support the funding from the European Research Council (ERC) under the European Union's Horizon 2020 research and innovation programme (Grant agreement No. 101098309 - PEBBLES).

References

[1] G. M. Voit, Reviews of Modern Physics **77**, 207 (2005)
[2] S. W.Allen *et al.*, ARA&A **49**, 409 (2011)
[3] R. A. Sunyaev & Y. B. Zeldovich, Comments on Astrophysics and Space Physics **4**, 173 (1972)
[4] Yu. N. Pariiskii, Soviet Ast. **16**, 1048 (1973)
[5] Planck Collaboration *et al.*, Astron. Astrophys. **594**, A27 (2016)
[6] L. E. Bleem *et al.*, Open J. Astrophys. **7**, 13 (2024)
[7] ACTDESHSC Collaboration *et al.*, arXiv e-prints arXiv:2507.21459 (2025)
[8] J. Tinker *et al.*, ApJ **688.2**, 709 (2008)
[9] L. Perotto *et al.*, Astron. Astrophys. **637**, A71 (2020)
[10] R. Adam *et al.*, Astron. Astrophys. **609**, A115 (2018)
[11] M. Calvo *et al.*, Journal of Low Temperature Physics, **184**, 816 (2016)
[12] D. Chérouvrier *et al.*, Astron. Astrophys. **700**, A30 (2025)
[13] M. Béthermin *et al.*, Astron. Astrophys. **607**, A89 (2017)
[14] M. Béthermin *et al.*, Astron. Astrophys. **667**, A156 (2022)
[15] A. A. Khostovan25 *et al.*, arXiv e-prints arXiv:2503.00120 (2025)
[16] J. R. Weaver *et al.*, ApJs **258.1**, 11 (2022)
[17] K. Kornoelje *et al.*, arXiv e-prints arXiv:2503.17271 (2025)
[18] M. Hilton *et al.*, ApJs **253.1**, 3 (2021)
[19] L. E. Bleem *et al.*, ApJs **247.1**, 25 (2020)
[20] L. E. Bleem *et al.*, ApJs **216.2**, 2 (2015)
[21] M. Fernández-Torreiro *et al.*, Highlights of Spanish Astrophysics XII, 8 (2025)